

Recent results and prospects from NA48/2: $K^\pm \rightarrow \pi^0 l^\pm \nu$ and $K^\pm \rightarrow \pi^+ \pi^- e^\pm \nu$, $K^\pm \rightarrow \pi^0 \pi^0 e^\pm \nu$ decays

Cristina Lazzeroni*

School of Physics and Astronomy, University of Birmingham, Birmingham B15 2TT, United Kingdom

Abstract

In 2003–2004 the NA48/2 Collaboration at CERN collected a large sample of K^\pm decays. Using data taken with minimal trigger conditions, a sample of 2.5×10^6 $K^\pm \rightarrow \pi^0 \mu^\pm \nu$ and 4.0×10^6 $K^\pm \rightarrow \pi^0 e^\pm \nu$ events was recorded, and allows precise measurements of the decay form factors. This report describes the event selection and the fitting procedure, and gives a preliminary result for the form factors in various parameterizations. In addition, with the full data sample collected, more than one million $K^\pm \rightarrow \pi^+ \pi^- e^\pm \nu$ and about 45000 $K^\pm \rightarrow \pi^0 \pi^0 e^\pm \nu$ decays has been analysed. An improved determination of the branching ratio and high precision form factor measurements for $K^\pm \rightarrow \pi^+ \pi^- e^\pm \nu$, and a preliminary result for the branching ratio of $K^\pm \rightarrow \pi^0 \pi^0 e^\pm \nu$ are presented in this paper. Future prospects include the observation of several thousands decays in similar muonic modes that will be studied at the NA62 experiment.

Keywords: NA48, Kaon, Semileptonic decays, Form factors, Branching ratio

1. Beam and detector

Simultaneous K^+ and K^- beams were produced by 400 GeV/c primary protons delivered by the CERN SPS and impinging on a beryllium target. The NA48/2 beamline selected kaons with a momentum range of (60 ± 3) GeV/c. A detailed description of the beamline and of the detector is available in [1]. The momentum of charged particles from K^\pm decays was measured by a magnetic spectrometer consisting of four drift chambers (DCH1–DCH4) and a dipole magnet between DCH2 and DCH3. Each chamber has eight planes of sense wires, two horizontal, two vertical and two along each of the orthogonal 45 degrees directions. The spectrometer is located in a tank filled with helium at atmospheric pressure and separated from the decay volume by a Kevlar window. A 16 cm diameter aluminium vacuum tube centred on the beam axis runs the length of the spectrometer through central holes in the window, drift

chambers and calorimeters. Charged particles are magnetically deflected in the horizontal plane by an angle corresponding to a transverse momentum kick of 120 MeV/c. The momentum resolution of the spectrometer is $\sigma(p)/p = 1.02\% \oplus 0.044\% p$ (p in GeV/c). The magnetic spectrometer is followed by a scintillator hodoscope. A liquid Krypton calorimeter (LKr) is used to measure the energy of electrons and photons. The calorimeter is $27 X_0$ thick and has an energy resolution $\sigma(E)/E = 0.032/\sqrt{E} \oplus 0.09/E \oplus 0.0042$ (E in GeV). The space resolution for single electromagnetic showers can be parameterised as $\sigma_x = \sigma_y = 0.42/\sqrt{E} \oplus 0.06$ cm for each transverse coordinate x, y . For the selection of muons, a muon veto system (MUV) was essential to distinguish muons from pions. It consisted of three planes of alternating horizontal and vertical scintillator strips. Each plane was shielded by a 80 cm thick iron wall. The inefficiency of the system was at the level of one per mil for muons with momentum greater than 10 GeV/c and the time resolution was below 1 ns.

*On behalf of the NA48 Collaboration

© CERN for the benefit of the NA48 Collaboration.

2. The $K^\pm \rightarrow \pi^0 l^\pm \nu$ decays

Semileptonic kaon decays (denoted as K_{l3} in the following, with $l = e, \mu$) provide the most accurate way and free of theoretical uncertainties, to measure the CKM matrix element $|V_{us}|$ [2]. To extract $|V_{us}|$, the knowledge of the decay form factors is crucial: since the form factors determine the Dalitz plot structure, both the detector acceptance (needed to measure the decay rate) and the phase space integral (needed to derive $|V_{us}|$ from the decay rate) heavily depend on the form factors. The hadronic matrix element of K_{l3} decays is described by two dimensionless form factors $f_\pm(t)$, which depend on the squared four-momentum $t = (p_K - p_\pi)^2$ transferred to the lepton system. The K^\pm decays are usually described in terms of the vector form factor f_+ and the scalar form factor f_0 defined as [2]:

$$f_0(t) = f_+(t) + \frac{t}{m_K^2 - m_\pi^2} f_-(t).$$

The functions f_+ and f_0 are related to the vector (1^-) and scalar (0^+) exchange to the lepton system, respectively. The contribution of f_- can be neglected in $Ke3$ decays since it is proportional to the lepton mass squared. By construction $f_0(0) = f_+(0)$. Since $f_+(0)$ is not directly measurable, it is customary to normalise all form factors to this quantity, so that:

$$\bar{f}_+(t) = \frac{f_+(t)}{f_0(t)}; \quad \bar{f}_-(t) = \frac{f_-(t)}{f_0(t)}.$$

To describe the form factors, two different parameterisations are used in this report. Widely known and most used is the Taylor expansion, called quadratic parameterisation in the following:

$$\bar{f}_{+,0}(t) = 1 + \lambda'_{+,0} \frac{t}{m_\pi^2} + \frac{1}{2} \lambda''_{+,0} \frac{t^2}{m_\pi^4}$$

where λ' and λ'' are the slope and the curvature of the form factors, respectively. The disadvantage of this parameterisation is related to the strong correlations between the parameters and the absence of a direct physical interpretation. To reduce the number parameters and to add a physical motivation, the pole parameterisation is used:

$$\bar{f}_+(t) = \frac{M_V^2}{M_V^2 - t}; \quad \bar{f}_0(t) = \frac{M_S^2}{M_S^2 - t}.$$

Here, the dominance of a single vector (V) or scalar (S) resonance is assumed and the corresponding pole mass M_V or M_S is the only free parameter.

The data used for the form factor analysis presented here were collected in 2004 during a dedicated run with a special trigger setup which required one or more tracks in the magnetic spectrometer and an energy deposit of at least 10 GeV/c in the electromagnetic calorimeter. Besides, the intensity of the beam was lowered and the momentum spread was reduced. The NA48 detector measures only the charged lepton and the two photons from the π^0 decay, while the neutrino leaves the detector unseen. To select the decay, one track in the magnetic spectrometer and at least two clusters in the electromagnetic calorimeter were required. The track had to be inside the geometrical acceptance of the detector, and needed a good reconstructed decay vertex, proper timing and a momentum greater than 5 GeV/c in case of electrons. For muons the momentum needed to be greater than 10 GeV/c to ensure high MUV efficiency. To identify the track as a muon, an associated hit in the MUV system and $E/p < 0.2$ was required, where E is the energy deposited in the LKr calorimeter and p is the track momentum. For electrons a range of $0.95 < E/p < 1.05$ and no associated hit in the MUV system were required. The neutral pions were reconstructed by two photon clusters in the LKr calorimeter, with an energy $E_\gamma > 3$ GeV/c, well isolated from any track hitting the calorimeter, and in time with the track in the spectrometer. Finally, the missing mass squared was required to satisfy $m_{miss}^2 < (10 \text{ MeV}/c^2)^2$ under a K^\pm hypothesis.

For K_{e3}^\pm , the only significant background is from $K^\pm \rightarrow \pi^\pm \pi^0$. A cut in the transverse momentum of the event reduces this background to less than 0.1% while losing only about 3% of the signal. For $K_{\mu 3}^\pm$ the background from $K^\pm \rightarrow \pi^\pm \pi^0$ with π^\pm decaying in flight is suppressed by using a combined requirement on the invariant mass $m(\pi^\pm \pi^0)$ (under π^\pm hypothesis) and on the π^0 transverse momentum. This cut reduces the contamination to 0.5%, but causes a loss of statistics of about 24%. Another background source is $K^\pm \rightarrow \pi^\pm \pi^0 \pi^0$ events with π^\pm decaying in flight and one π^0 not reconstructed. Its contribution is estimated to be only about 0.1% and therefore no specific cut was applied. To extract the form factors, two-dimension fits to the Dalitz plot densities $\rho(E_l^*, E_\pi^*)$ are performed:

$$\begin{aligned} \rho(E_l^*, E_\pi^*) &= \frac{d^2 N(E_l^*, E_\pi^*)}{dE_l^* dE_\pi^*} \\ &\approx A f_+^2(t) + B f_+(t)(f_+(t) - f_0(t)) \frac{m_K^2 - m_\pi^2}{t} \\ &\quad + C [(f_+(t) - f_0(t)) \frac{m_K^2 - m_\pi^2}{t}]^2 \end{aligned}$$

To obtain the lepton and pion energies E_l^* and E_π^* in the kaon rest frame, the reconstructed lepton and pion four-momenta are boosted into the kaon rest frame. The kaon energy is computed from the decay products, assuming no transverse component of the momentum of the kaon. This leaves two solutions for the longitudinal component of the neutrino momentum, from which the one closer to 60 GeV/c is used. In this way the energy resolution in the Dalitz plot, in particular for high pion energies, is greatly improved. The reconstructed Dalitz plots are then corrected for remaining background, detector acceptance and distortions induced by radiative effects. The radiative effects are simulated by using a special Monte Carlo generator developed by the KLOE collaboration[3]. This generator gives the same corrections as a recent calculation within Chiral Perturbation Theory with fully inclusive real photon emission[4]. For the purpose of the fit, the Dalitz plots were subdivided into cells of 5 MeV \times 5 MeV; cells which crossed or are outside the kinematical borders are not used in the fit. The fit results for the quadratic and the pole parameterisations are listed in Tables 1 and 2. The systematic uncertainties are evaluated by changing the cuts defining the vertex quality and the geometrical acceptance by small amounts. In addition, variations to the resolutions of pion and muon energies in the kaon centre of mass system are applied; the pion decay background is varied and the differences in the results of two independent analyses done in parallel are taken into account. For comparison the combined $K_{\beta 3}^\pm$ quadratic fit results as reported by recent experiments[2] are shown in Fig. 1. The 68% confidence level contours are displayed for both neutral (KLOE, KTeV and NA48) and charged decays (ISTRA+ studied K^- only). The preliminary NA48/2 results presented here are the first high precision measurements done with both K^+ and K^- mesons. The form factors are in good agreement with the measurements done by the other experiments (except the neutral channel from NA48[5]) and compatible with the combined fit done by FlaviaNet[2].

	$\lambda'_+ [10^{-3}]$	$\lambda''_+ [10^{-3}]$	$\lambda^0_+ [10^{-3}]$
K_{e3}^\pm	$27.2 \pm 0.7 \pm 1.1$	$0.7 \pm 0.3 \pm 0.4$	
$K_{\mu 3}^\pm$	$26.3 \pm 3.0 \pm 2.2$	$1.2 \pm 1.1 \pm 1.1$	$15.7 \pm 1.4 \pm 1.0$
tot	27.0 ± 1.1	0.8 ± 0.5	16.2 ± 1.0

Table 1: Preliminary form factor fit results for the quadratic with statistical and systematic uncertainties. For the combined (tot) result both uncertainties were combined.

	$M_V [\text{MeV}/c^2]$	$M_S [\text{MeV}/c^2]$
K_{e3}^\pm	$879 \pm 3 \pm 7$	
$K_{\mu 3}^\pm$	$873 \pm 8 \pm 9$	$1183 \pm 31 \pm 16$
tot	877 ± 6	1176 ± 31

Table 2: Preliminary form factor fit results for the pole parameterizations with statistical and systematic uncertainties. For the combined (tot) result both uncertainties were combined.

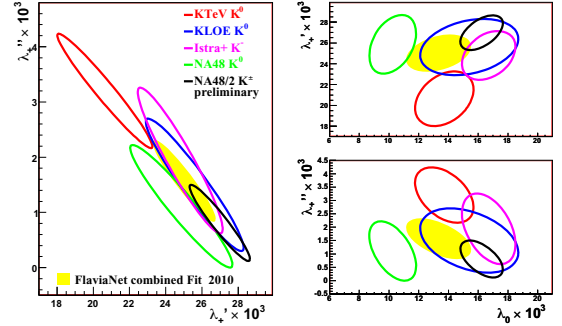


Figure 1: Combined quadratic fit results for KL3 decays. The ellipses are 68% confidence level contours. For comparison the combined fit from the FlaviaNet kaon working group is shown [2].

3. The $K^\pm \rightarrow \pi^+\pi^-e^\pm\nu$ decays

The kinematics of the $K^\pm \rightarrow \pi^+\pi^-e^\pm\nu$ decay is described by the five Cabibbo-Maksymowicz variables [6]: the square of the di-pion invariant mass S_π , the square of the di-lepton invariant mass S_e , the angle θ_π of the π^\pm in the di-pion rest frame with respect to the flight direction of di-pion in the kaon rest frame, the angle θ_e of the e^\pm in the di-lepton rest frame with respect to the flight direction of di-lepton in the kaon rest frame, and the angle Φ between the di-pion and di-lepton planes in the kaon rest frame. The decay amplitude is the product of the leptonic weak current and the hadronic current. The hadronic current is described in terms of three (F, G, R) axial- vector and one (H) vector complex form factors. The sensitivity of the decay matrix element to the form factor R is negligible due to the small mass of the electron. These form factors may be developed in a partial wave expansion with respect to the variable $\cos\theta_\pi$:

$$\begin{aligned}
 F &= F_s e^{i\delta_{fs}} + F_p e^{i\delta_{fp}} \cos\theta_\pi + F_d e^{i\delta_{fd}} \cos^2\theta_\pi + \dots \\
 G &= G_p e^{i\delta_{gp}} \cos\theta_\pi + G_d e^{i\delta_{gd}} \cos^2\theta_\pi + \dots \\
 H &= H_p e^{i\delta_{hp}} \cos\theta_\pi + H_d e^{i\delta_{hd}} \cos^2\theta_\pi + \dots
 \end{aligned}$$

Limiting the expansion to S- and P-waves and considering a unique phase δ_p for all P-wave form factors in absence of CP violating weak phases, one will obtain the decay probability, that depends only on the form factor magnitudes F_s, F_p, G_p, H_p , the single phase difference $\delta = \delta_s - \delta_p$ and kinematic variables. The form factors can be expressed as a series expansion of the dimensionless invariants $q^2 = (S_\pi/4m_\pi^2) - 1$ and $S_e/4m_\pi^2$ [7]. Two slope and one curvature terms are sufficient to describe the measured F_s form factor variation within the available statistics:

$$F_s/f_s = 1 + f'_s/f_s q^2 + f''_s/f_s q^4 + f'_e S_e/f_s 4m_\pi^2$$

while two terms are enough to describe the G_p form factor:

$$G_p/f_s = g_p/f_s + g'_p/f_s q^2$$

and two constants to describe the F_p and H_p form factors. A high precision measurement of the normalised form factor parameters (divided by f_s as shown above) has been published by NA48/2 [8]. The measurement of their absolute values requires the measurement of the branching fraction. Recently a new measurement of the $K^\pm \rightarrow \pi^+\pi^-e^\pm\nu$ branching ratio by NA48/2 has been published in [9]. Here only a summary description of the measurement is given.

The $K^\pm \rightarrow \pi^+\pi^-e^\pm\nu$ rate is measured relative to $K^\pm \rightarrow \pi^+\pi^+\pi^-$ normalization channel. The two samples were collected concurrently using the same trigger. The branching ratio (BR) is obtained as

$$BR(K_{e4}^\pm) = \frac{N_s - N_b}{N_n} \frac{A_n \epsilon_n}{A_s \epsilon_s} BR(K_{3\pi})$$

where N_s, N_b and N_n are the numbers of signal, background and normalization candidates. A_s and ϵ_s are the acceptance and trigger efficiency for the signal sample, while A_n and ϵ_n are those for the normalization events. The signal and normalization data samples were selected if having three reconstructed charged tracks in time with the corresponding hodoscope signals. The three-track reconstructed vertex of the ± 1 total charge was required to lie within 5 cm of the beam axis, and its longitudinal position was required to be between 2 m and 95 m downstream of the final collimator. The maximum momentum sum was set at 70 GeV/c. All vertex tracks were required to be within the spectrometer, hodoscope, LKr and muon veto acceptances. The distance between any two tracks at DCH1 was required to be larger than 2 cm, and the distance between any track and the beam mean position (monitored with a separate sample of $K^\pm \rightarrow \pi^+\pi^+\pi^-$ decays) was larger than 12 cm. The minimum distance between the track

impact at the LKr front face and the nearest LKr dead cell was required to be at least 2 cm. The track-to-track distance at the LKr front face had to be larger than 20 cm to prevent shower overlaps. No in-time track-associated hits were allowed in two planes of the muon veto. The vertex with the lowest fit χ^2 was selected. A track with $p > 2.75$ GeV and $0.9 < E/p < 1.1$ was identified as electron/positron, while the track with $p > 5$ GeV and $E/p < 0.8$ was regarded as a pion. A cut on the value of a dedicated linear discriminant variable based on shower properties has been applied, to reject events with one misidentified pion. Kaon candidates were then selected among the vertices with a single electron/positron candidate and a pair of opposite-charged pions. To suppress the $K^\pm \rightarrow \pi^\pm\pi^+\pi^-$ background, the vertex invariant mass $M_{3\pi}$ in the $\pi^\pm\pi^+\pi^-$ hypothesis and its transverse momentum were required to be outside an ellipse centred at the PDG kaon mass [10] and zero transverse momentum, with semi-axes of 20 MeV/c² and 35 MeV/c, respectively. The square missing mass of $K^\pm \rightarrow \pi^\pm X$ decay was required to be larger than 0.04 (GeV/c²)² to reject $\pi^\pm\pi^0$ decays with a subsequent $\pi^0 \rightarrow e^+e^-\gamma$ process. The invariant mass of any possible electron-positron system was required to be more than 0.03 GeV/c² in order to reject photon conversions. For $K^\pm \rightarrow \pi^+\pi^-e^\pm\nu$ events, the reconstruction of the kaon momentum assuming a four-body decay with the undetected neutrino was implemented, and the solution closer to 60 GeV/c was chosen. For the normalization channel the vertex was required to be composed of three charged pions. $M_{3\pi}$ and transverse momentum were required to be inside an ellipse with semi-axes 12 MeV/c² and 25 MeV/c, respectively. Events with reconstructed kaon momentum between 54 and 66 GeV/c were kept for further analysis. A total sample of about 1.1 million candidates and about 19 millions of prescaled normalization candidates were selected from data recorded in 2003-2004.

There are two main background sources: $K^\pm \rightarrow \pi^\pm\pi^+\pi^-$ decays with subsequent $\pi \rightarrow e\nu$ decay or a pion mis-identified as an electron; and $K^\pm \rightarrow \pi^0(\pi^0)\pi^\pm$ with subsequent $\pi^0 \rightarrow e^+e^-\gamma$ decay with undetected photons and an electron mis-identified as a pion. The background contamination was estimated from the wrong sign events (two same sign pions), which can only be background. To estimate the right sign part of the background in the selected sample, the number of wrong sign events were multiplied by 2, as the dominant contribution comes from $K^\pm \rightarrow \pi^\pm\pi^+\pi^-$ decays, as is confirmed by Monte Carlo simulation. The total background contribution is below 1%. A detailed GEANT3-based Monte Carlo simulation was used to take into ac-

count full detector geometry, DCH alignment, local inefficiencies and beam properties. Sources of systematic uncertainties include acceptance stability, muon veto efficiency, accidental activity in detectors, particle identification, background estimate procedure, radiative effects modelling, trigger efficiency and Monte Carlo simulation statistical error.

The resulting branching fraction is measured to be 3 times more precise than the current value [10]:

$$BR(K^\pm \rightarrow \pi^+ \pi^- e^\pm \nu) = (4.257 \pm 0.004_{stat} \pm 0.016_{syst} \pm 0.031_{ext}) \times 10^{-5}.$$

The external error, caused by the uncertainty of the normalization channel branching fraction, is the dominant error of the measurement. The measured branching fraction has been used to extract the normalization form factor $f_s = 5.705 \pm 0.003_{stat} \pm 0.017_{syst} \pm 0.031_{ext}$ and all the absolute values of hadronic form factor parameterization constants are shown in Table 3. Normalization errors are fully correlated. A large anticorrelations exist between f' and f'' (-0.954) as well as between g_p and g'_p (-0.914).

	value	Stat.	Syst.	Norm.
f'_s	0.867	0.040	0.029	0.005
f''_s	-0.416	0.040	0.034	0.003
f'_e	0.388	0.034	0.040	0.002
f_p	-0.274	0.017	0.023	0.002
g_p	4.952	0.057	0.057	0.031
g'_p	0.508	0.097	0.074	0.003
h_p	-2.271	0.086	0.046	0.014

Table 3: Form factors with statistical, systematic and normalization uncertainties, after using the measurement of f_s .

4. The $K^\pm \rightarrow \pi^0 \pi^0 e^\pm \nu$ decays

For $K^\pm \rightarrow \pi^0 \pi^0 e^\pm \nu$ decays, due to restrictions of symmetry, the matrix element does not depend on θ_π and Φ angles, and it is parametrized just in terms of the only form factor F_s that in the general case may depend on S_π and S_e . The rate is measured relative to $K^\pm \rightarrow \pi^0 \pi^0 \pi^\pm$ normalization channel. These two samples are collected with the same trigger of high efficiency for the corresponding event topology. A common event selection was considered as far as possible. Events with at least four γ s detected by LKr, and at least one track, reconstructed from spectrometer data, were regarded as candidates. Every combination of two γ

pairs, detected by LKr, was considered as a pair of π^0 s. Reconstructed longitudinal positions of both $\pi^0 \rightarrow \gamma\gamma$ decay candidates were required to coincide within 500 cm, and their average position Z_n to be in the fiducial volume. Decay longitudinal position Z_{ch} , assigned to every track, was defined as the closest distance approach between the track and the beam axis. A combined vertex, composed of four LKr clusters and one charged track, was required to have the difference between these two measured longitudinal positions $|Z_n - Z_{ch}|$ less than 800 cm. Pion and electron identification was the same as in charged case.

The $K^\pm \rightarrow \pi^0 \pi^0 e^\pm \nu$ and $K^\pm \rightarrow \pi^0 \pi^0 \pi^\pm$ decays were discriminated by means of elliptic cuts in the $(M_{\pi^0 \pi^0 \pi^\pm}, p_t)$ plane, where $M_{\pi^0 \pi^0 \pi^\pm}$ is the invariant mass of the combined vertex in the 3π hypothesis, and p_t is the transverse momentum. The elliptic cut separates about 70 million normalization events from 45000 $K^\pm \rightarrow \pi^0 \pi^0 e^\pm \nu$ candidates. The residual fake-electron background is estimated to be about 1.3% of the signal. Background from $K^\pm \rightarrow \pi^0 \pi^0 \pi^\pm$ with the subsequent $\pi^\pm \rightarrow e^\pm \nu$ is only 0.1% of the signal. For the calculation of the $K^\pm \rightarrow \pi^0 \pi^0 \pi^\pm$ acceptance, the NA48/2 empirical parameterization of its Dalitz plot [11] has been used. For the $K^\pm \rightarrow \pi^0 \pi^0 e^\pm \nu$ decay mode, the NA48/2 result [12] for F_s parameterization has been used, since it well describes also $K^\pm \rightarrow \pi^0 \pi^0 e^\pm \nu$ decays for $S_\pi > (2m_{\pi^\pm})^2$.

Following the notation described in the previous section, and using the obtained acceptance values $A_s = 1.77\%$ and $A_n = 4.11\%$ and the value of the normalization channel branching fraction from [10], the preliminary result has been obtained:

$$BR(K^\pm \rightarrow \pi^0 \pi^0 e^\pm \nu) = (2.595 \pm 0.012_{stat} \pm 0.024_{syst} \pm 0.032_{ext}) \times 10^{-5}.$$

This measurement is 10 times more precise than the current PDG corresponding value [10]. Systematic errors include the contributions from background uncertainty, simulation statistical error, sensitivity to form factors, radiative corrections, trigger efficiency and beam geometry uncertainties. The external error comes from the uncertainty on the normalization channel branching fraction.

5. Future prospects

The NA62 experiment, using the same beam line and detector of NA48/2, collected data in 2007 to perform tests of Lepton Flavour Universality. The collected data sample contain about $40 \times 10^6 K_{e3}^+$ and $20 \times 10^6 K_{\mu 3}^+$

events, respectively. A special K_L run was also taken, providing further K_{e3}^0 and $K_{\mu3}^+$ samples of about 4×10^6 events each. Therefore NA62 will be able to achieve an higher statistical precision measurements of the form factors of all K_{l3} channels as available already today.

Improved measurements of $K^\pm \rightarrow \pi^+\pi^-e^\pm\nu$ and $K^\pm \rightarrow \pi^0\pi^0e^\pm\nu$ branching ratios have been presented here. The study of the form factors for the neutral channel is in progress and will complete the high-precision picture of $K^\pm \rightarrow \pi\pi e^\pm\nu$ decays. While the above analyses are published or close to completion and should appear shortly in final publications, future prospects include the observation of several thousand decays in similar muonic modes: $K^\pm \rightarrow \pi^0\pi^0\mu^\pm\nu$ (never observed) and $K^\pm \rightarrow \pi^+\pi^-\mu^\pm\nu$ (7 events observed) [13]. Such poorly known modes could be studied also in the forthcoming NA62 experiment currently under construction.

References

- [1] V. Fanti et al., Nucl. Instrum. Meth. A574 (2007) 433-471.
- [2] M. Antonelli et al., E. Phys. J. C 69 (2010) 399.
- [3] C. Gatti, E. Phys. J C 45 (2006) 417.
- [4] V. Cirigliano, M. Giannotti, H. Neufeld, JHEP 11 (2008) 006.
- [5] A. Lai et al., Phys. Lett. B 647 (2007) 341.
- [6] N. Cabibbo, A. Maksymowicz, Phys. Rev. 137 (1965) 438-443.
- [7] G. Amoros, J. Bijnens, J. Phys. G 25 (1999) 1607-1622.
- [8] J. Batley et al., Eur. Phys. J. C 64 (2009) 589-608.
- [9] J. Batley et al., Phys. Lett. B 715 (2012) 105-115.
- [10] Review of Particle Physics (RPP), Phys. Rev. D 86 (2012) 010001.
- [11] J. Batley et al., Phys. Lett. B 686 (2010) 101-108.
- [12] J. Batley et al., Eur. Phys. J. C 70 (2010) 635-657.
- [13] V. Bisi, R. Cester, A. Marzari-Chiesa, M. Vigone, Phys. Lett. B 25 (1967) 572.